Retention and Remobilization of Stabilized Silver Nanoparticles in an Undisturbed Loamy Sand Soil

ARTICLE *in* ENVIRONMENTAL SCIENCE & TECHNOLOGY · OCTOBER 2013

Impact Factor: 5.33 · DOI: 10.1021/es402046u · Source: PubMed

6 AUTHORS, INCLUDING:

Jiri, Jirka Simunek
University of California, Riverside
375 PUBLICATIONS **9,430** CITATIONS

SEE PROFILE

Environmental Science & Technology

Article

pubs.acs.org/est

Retention and Remobilization of Stabilized Silver Nanoparticles in an Undisturbed Loamy Sand Soil

Yan Liang,[†] Scott A. Bradford,*[,‡] Jiri Simunek,[§] Marc Heggen,[∥,⊥] Harry Vereecken,[†] and Erwin Klumpp[†]

[†]Agrosphere Institute IBG-3, Forschungszentrum Jülich GmbH, Jülich 52425, Germany

[‡]United States Department of Agriculture, Agricultural Research Service, U. S. Salinity Laboratory, Riverside, California United States

[§]Department of Environmental Sciences, University of California, Riverside, California United States

[∥]Peter Grünberg Institute PGI-5, Jülich 52425, Germany

[⊥]Ernst Ruska-Centrum ER-C, Forschungszentrum Jülich GmbH, Jülich 52425, Germany

Supporting Information

ABSTRACT: Column experiments were conducted with undisturbed loamy sand soil under unsaturated conditions (around 90% saturation degree) to investigate the retention of surfactant stabilized silver nanoparticles (AgNPs) with various input concentration (C_o), flow velocity, and ionic strength (IS), and the remobilization of AgNPs by changing the cation type and IS. The mobility of AgNPs in soil was enhanced with decreasing solution IS, increasing flow rate and input concentration. Significant retardation of AgNP breakthrough and hyperexponential retention profiles (RPs) were observed in almost all the transport experiments. The retention of AgNPs was successfully analyzed using a numerical model that accounted for time- and depth-dependent retention. The simulated retention rate coefficient (k_1) and maximum retained concentration on the solid phase (S_{max}) increased with increasing IS and decreasing C_o. The high k_1 resulted in retarded breakthrough curves (BTCs) until S_{max} was filled and then high effluent concentrations were obtained. Hyperexponential RPs were likely caused by the hydrodynamics at the column inlet which produced a concentrated AgNP flux to the solid surface. Higher IS and lower C_o produced more hyperexponential RPs because of larger values of S_{max}. Retention of AgNPs was much more pronounced in the presence of Ca^{2+} than K^+ at the same IS, and the amount of AgNP released with a reduction in IS was larger for K^+ than Ca^{2+} systems. These stronger AgNP interactions in the presence of Ca^{2+} were attributed to cation bridging. Further release of AgNPs and clay from the soil was induced by cation exchange (K^+ for Ca^{2+}) that reduced the bridging interaction and IS reduction that expanded the electrical double layer. Transmission electron microscopy, energy-dispersive X-ray spectroscopy, and correlations between released soil colloids and AgNPs indicated that some of the released AgNPs were associated with the released clay fraction.

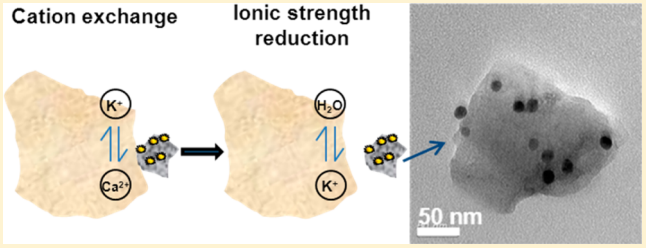

INTRODUCTION

The transport and fate of nanoparticles (NPs) in the subsurface environment has been a topic of significant scientific interest[1] because soils and aquifers act as the primary filter systems to protect water resources. NPs have sometimes been found to be highly mobile under environmentally relevant conditions[2−4] and may potentially contaminate groundwater. Colloid and NP mobility in the subsurface environment are generally considered to be determined by physicochemical interactions and size-related processes.[5−7] Retention of colloids/NPs in porous media is controlled by the coupling of physicochemical properties of the particle and the collector surface, solution chemistry, and hydrodynamics of the system.[8,9] Filtration theory[10] has commonly been employed to predict the deposition of NPs on collector surfaces. However, deviations from filtration theory predictions have frequently been demonstrated, e.g., the production of asymmetric or retarded breakthrough curves (BTCs) and uniform, nonmonotonic, and hyperexponential retention profiles (RPs).[11,12] Remobilization of deposited colloids/NPs from solid to aqueous phases has received only limited attention. Existing data indicate that release may occur with an increase in the hydrodynamic force[13] or a reduction in the adhesive force.[14] In particular, decreasing the solution ionic strength (IS)[5,15] and/or replacement of divalent cations by monovalent cations[16] can induce colloid/NP release by reducing the depth of the secondary energy minimum and cation bridging, respectively.

Most research studies have investigated NP/colloid transport in highly idealized systems consisting of repacked, homogeneous, coarse textured porous media under water-saturated[3,5,17] or unsaturated condition.[18−20] This previous research has provided fundamental knowledge and understanding of the influence of many physicochemical factors on NP transport and

Received: May 7, 2013
Revised: September 23, 2013
Accepted: October 9, 2013
Published: October 9, 2013

Table 1. Experimental Parameters and the Mass Recovery for Column Experiments[a]

	C_o (mg L^{-1})	q (cm min^{-1})	IS (mM)	φ	θ_w	λ	recovery, % M_{eff}	M_{sand}	M_{total}
Figure 1	10	0.006	1	0.431	0.407	0.944	37.9	70.5	108.4
	10	0.006	5	0.453	0.429	0.947	13.9	78.7	92.6
	10	0.006	10	0.452	0.407	0.900	3.4	88.6	92.0
Figure 2	10	0.006	1	0.431	0.407	0.944	37.9	70.5	108.4
	1	0.006	1	0.462	0.438	0.949	14.4	96.2	110.6
Figure 3	10	0.02	1	0.467	0.397	0.851	64.3	40.0	104.3
	10	0.006	1	0.431	0.407	0.944	37.9	70.5	108.4

			IS_A (mM)	M_A	M_B H_2O	IS_C (mM)	M_C	M_D H_2O	IS_E (mM)	M_E	M_F H_2O
Figure 4	III, 10	0.02	10, Ca^{2+}	<1%	16.0						
	IV, 10	0.02	10, K^+	9.1	31.7						
Figure 5a	I, 10	0.02	1, Ca^{2+}	3.9	3.8	1, K^+	<1%	1.5	100, K^+	5.0	9.4
	II, 10	0.02	5, Ca^{2+}	<1%	4.6	5, K^+	<1%	10.8	100, K^+	<1%	7.7
	III, 10	0.02	10, Ca^{2+}	<1%	16.0	10, K^+	<1%	16.7	100, K^+	<1%	4.2

[a]Figure 1 ionic strength effect; Figure 2: concentration effect; Figure 3: flow rate effect; Figure 4: release of AgNPs by ionic strength reduction; Figure 5a: release of AgNPs by cation exchange and ionic strength reduction; C_o, AgNP input concentration; q, Darcy velocity; IS, ionic strength; φ, porosity; θ_w: water content; λ, water saturation; M_{eff}, M_{sand}, and M_{total} are mass percentages recovered from effluent, sand, and total, respectively; $M_A - M_F$ are the mass percentages recovered from Steps A−F in release experiments.

deposition. However, simplified porous media such as glass beads and clean sands are not able to account for the full complexity and heterogeneity of natural soils (e.g., pronounced surface roughness, highly nonuniformed soil particle size distributions, the complex pore structure of soil, and surface chemical heterogeneity due to a wide variety of inorganic and organic compounds). Previous studies concerning the mobility of colloids/NPs in soil[6,7,21] have indicated that the pore structure and soil properties strongly affect particle retention in the subsurface environment. In addition, the presence of different electrolyte types, which generally occurs in soils, has been proven to play an important role in NP stability and mobility in porous media.[7,22,23] In particular, divalent cations can enhance aggregation and deposition in comparison to monovalent ions.[6,24]

The environmental fate of silver nanoparticles (AgNPs) is of special concern because of their strong antimicrobial activity, and considerable amounts of research have therefore addressed this issue.[2,25−31] Previous studies have indicated that the interaction of AgNPs and sand is controlled by physicochemical conditions of the system.[2,25,26] The surface modification of AgNPs and the presence of stabilizers significantly influenced their transport behavior under environmental conditions and potentially extended their toxicity in ecosystems.[26,31−33] Heterogeneity on the collector surface strongly influenced AgNP transport.[25,33] In particular, we recently demonstrated in column studies that some of the AgNPs interacted with quartz sand in a weak secondary minimum, while other AgNPs strongly interacted in a primary minimum due to microscopic heterogeneity. The breakthrough curves exhibited blocking behavior (a decreasing retention rate with time) as the maximum retained concentration on the solid phase (S_{max}) filled.[33] Furthermore, RP shapes transitioned from hyperexponential, to nonmonotonic, and to uniform during blocking as S_{max} was filled by retained AgNPs and free surfactant molecules.[33] Mechanical straining and chemical interactions between AgNPs and the soil surface have also been suggested to play important roles in AgNP retention in a disturbed sandy soil.[7] Studies on the mobility of micrometer-sized colloids pointed out that the pore structure of undisturbed soil and leaching of naturally occurring particles during infiltration were important processes that affected contaminant migration.[21,34] To date, no studies have reported on the transport, retention and remobilization of AgNPs in undisturbed and/or unsaturated soil systems. In particular, the potential of AgNPs cotransported by natural soil colloids has not yet been studied.

The objective of this study is to better understand the retention and remobilization behavior of stabilized AgNPs in a natural soil, near water saturation (90%) conditions to represent the maximum transport potential in the vadose zone. Undisturbed soil column experiments were conducted for different solution chemistries, input AgNP concentrations, and flow velocities, and a mathematical model was employed to quantitatively assess the effects of these physicochemical factors on retention. Following AgNP transport and retention, release experiments were performed by systematically changing the IS and cation type of the eluting solution. Results provide valuable insight on the transport, retention, and release behavior of AgNPs in a natural soil over a range of environmentally relevant conditions. This information is needed to better assess the risk of AgNP exposure to ecosystems and to develop strategies for waste management and remediation.

MATERIALS AND METHODS

Below we summarize experimental procedures and protocols. Additional details are provided in the Supporting Information, SI.

AgNPs and Solution Chemistry. The preparation and characterization of AgNP suspensions have been described in our previous study.[33] Briefly, surface stabilized AgNPs (AgPURE) were produced using a mixture of two nonionic surfactants, polyoxyethylene glycerol trioleate and polyoxyethylene (20) sorbitan mono-laurate (Tween 20) at 4% w/w for each. Analyses of transmission electron microscopy images indicated that the AgNPs were spherical in shape and around 99% of the AgNPs were in the size range of 15−20 nm. Electrolyte solutions were made using Milli-Q water and KNO_3 or $Ca(NO_3)_2$, and the pH ranged from 6 to 7 during the course of the transport experiments. The surface charge characteristics and size of AgNPs in a selected electrolyte solution were determined using a Nano-Zetasizer apparatus (Malvern ZetaSizer 4).

Soil. Polyvinyl chloride columns (8 cm in inner diameter and 10 cm in length) were filled with undisturbed soil from the upper 30 cm of an agricultural field (Kaldenkirchen, North-rhine-Westphalia, Germany). Soil samples were analyzed for specific properties. The soil was classified as a loamy sand, with 4.9% clay (<0.002 mm), 26.7% silt (0.002−0.064 mm), and 68.5% sand (0.064−2.000 mm).[35] This soil had a total organic matter content of 1.1%,[35] a cationic exchange capacity of 7.8 $cmol_c\ kg^{-1}$,[36] and a specific surface area of 1.7 $m^2\ g^{-1}$. The clay fraction contains the clay minerals illite, montmorillonite, and kaolinite. The surface charge characteristics of the soil in a selected electrolyte solution were determined using a Nano-Zetasizer apparatus (Malvern ZetaSizer 4).

Transport Experiments. AgNP transport experiments were conducted at different IS (1, 5, and 10 mM), input concentration values (C_o, 1 and 10 mg/L), and Darcy water velocities (q, 0.02 and 0.006 cm/min) by injecting a pulse (around 2 pore volumes) of AgNP suspension into the column. A 90% water-saturation was employed in these experiments to reflect the influence of entrapped air on water flow in the vadose zone. A summary of the experimental conditions is provided in Table 1. After recovery of the AgNP breakthrough curve (the C/C_o value less than 0.5%), the soil from the column was carefully excavated in approximately 1 cm increments, and then freeze-dried. BTCs and RPs for AgNPs were obtained from concentrations of Ag in the effluent and soil samples, respectively, which were digested in HNO_3 and then determined by an inductively coupled plasma mass spectrometer (ICP-MS, Agilent 7500ce). Each sample was measured three times, and the average value was taken for analysis. The dissolution of AgNPs was determined to be negligible in this study. Consequently, Ag concentrations were directly related to the number of AgNPs in the sample.

AgNP Release Experiments . A series of experiments was performed to deduce the effects of cation type and concentration, IS reduction, and cation exchange on the release of AgNPs. The input concentration of AgNPs was 10 mg/L and the Darcy velocity was 0.02 cm/min for all the release experiments. Four different solution chemistry conditions were considered for the initial AgNP deposition and elution with AgNP free solution (step A), namely: 0.333 mM $Ca(NO_3)_2$ (experiment I); 1.65 mM $Ca(NO_3)_2$ (experiment II); 3.33 mM $Ca(NO_3)_2$ (experiment III); and 10 mM KNO_3 (experiment IV). Similar to the AgNP transport experiments described in the preceding section, the IS was 1, 5, 10, and 10 mM for experiments I, II, III, and IV, respectively. The release experiments I−III were subsequently conducted using the following elution solution chemistry sequence: Milli-Q water (step B); KNO_3 at the same IS as in step A (step C); Milli-Q water (step D); 100 mM KNO_3 (step E); and Milli-Q water (step F). Experiment IV consisted of only steps A and B. Concentrations of Ag, K, Ca, Fe, and Al in select effluent samples were measured using inductively coupled plasma mass spectrometry/optical emission spectrometry (ICP-MS/OES). Concentrations of K and Ca demonstrate the process of cation exchange. Concentrations of Fe and Al reflect the amount of released soil colloids in the effluent. Additional analysis of selected effluent samples was conducted, including: zeta potential, transmission electron microscopy (TEM) (Philips CM 20 FEG), and energy-dispersive X-ray spectroscopy (EDX) (EDAX, Genesis).

Mathematical Model. A one-dimensional form of the convection-dispersion equation was used to simulate the AgNP transport and retention in the undisturbed soil columns as follows:

$$\frac{\partial(\theta_w C)}{\partial t} = \frac{\partial}{\partial z}\left(\theta_w D \frac{\partial C}{\partial z}\right) - \frac{\partial(qC)}{\partial z} - \theta_w \psi k_1 C \quad (1)$$

$$\frac{\partial(\rho_b S)}{\partial t} = \theta_w \psi k_1 C \quad (2)$$

where θ_w [−] is the volumetric water content, C [M L^{-3}, M and L denote units of mass and length, respectively] is the aqueous phase AgNP concentration, t is time [T, T denotes time units], z [L] is the distance from the column inlet, D [L^2T^{-1}] is the hydrodynamic dispersion coefficient, q [L T^{-1}] is the Darcy water flux, ψ [−] is a dimensionless function to account for time- and depth-dependent blocking, k_1 [T^{-1}] is the first-order retention coefficient of AgNPs from the aqueous to the solid phase, ρ_b [M L^{-3}] is the soil bulk density, and S [M M^{-1}] is the AgNP concentration on the solid phase. The ψ term is given as follows: [37]

$$\psi = \left(1 - \frac{S}{S_{max}}\right)\left(\frac{d_{50} + z}{d_{50}}\right)^{-\beta} \quad (3)$$

where d_{50} [L] is the median grain size of the porous medium, β [−] is an empirical parameter controlling the shape of the spatial distribution of retained NPs, and S_{max} [M M^{-1}] is the maximum solid phase concentration of deposited AgNPs. In this study, β = 1.532 was chosen for simulation instead of 0.432 that was applied in AgNP transport in sand.[33] The first term on the right side of eq 3 accounts for time dependent blocking/filling of retention sites using a Langmuirian approach,[38] while the second term on the right side describes depth dependent retention (e.g., a decreasing retention rate with depth).

The pore water velocity and dispersivity in the AgNP transport simulations were determined from the tracer BTCs by fitting to the solution of the advection dispersion equation. The parameters k_1 and S_{max} were obtained from the observed AgNP transport and retention using the inverse fitting algorithm[39] in HYDRUS-1D.[40] A third type boundary condition and zero dispersive flux were set for the column inlet and outlet, respectively, for all simulations. The release experiments were not simulated because of the confounding influence of clay release.

RESULTS AND DISCUSSION

AgNP and Soil Properties. The size of AgNPs in IS of 1 to 100 mM KNO_3 and $Ca(NO_3)_2$ were in the range of 45 to 78 nm without an obvious trend. The zeta potentials of the AgNPs and soil in the same IS range are presented in SI Figure S1. The zeta potentials of AgNPs were negative and did not vary much over the considered conditions. The zeta potentials of the soil exhibited much more negative charges than the AgNPs.

AgNP Transport and Retention in Undisturbed Soil. Figures 1−3 show the observed and simulated BTCs and RPs for AgNPs in the undisturbed soil for various IS (Figure 1), input concentrations (Figure 2), and flow velocities (Figure 3). Here BTCs are plotted as normalized effluent concentrations (C/C_o) versus eluted pore volumes, and RPs are plotted as normalized solid phase concentrations (S/C_o) with distance from the column inlet. Mass balance information for the BTCs, RPs, and total columns are provided in Table 1. The total column mass balance (92−111%) was very good. SI Table S1

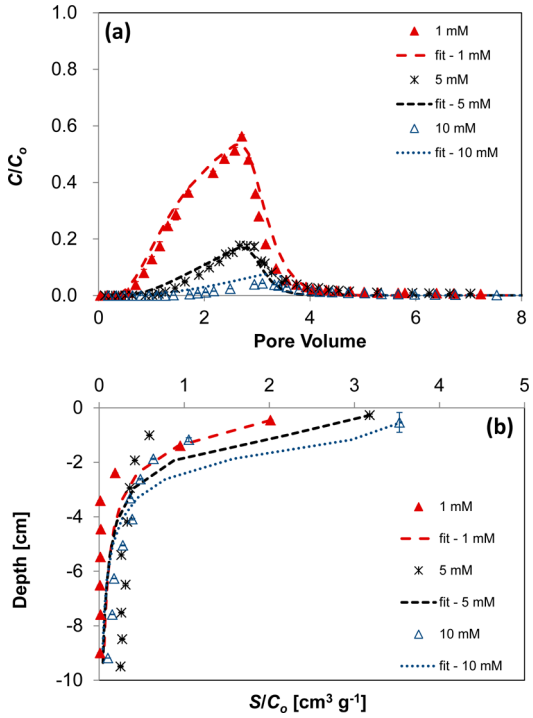

Figure 1. Effect of ionic strength on the transport and retention of AgNPs in an undisturbed loamy sand soil: observed and fitted breakthrough curves (a) and retention profiles (b) of AgNPs under 1, 5, and 10 mM KNO_3, respectively. Other experimental conditions were the same: input concentration, 10 mg/L AgNPs; Darcy velocity, 0.006 cm/min.

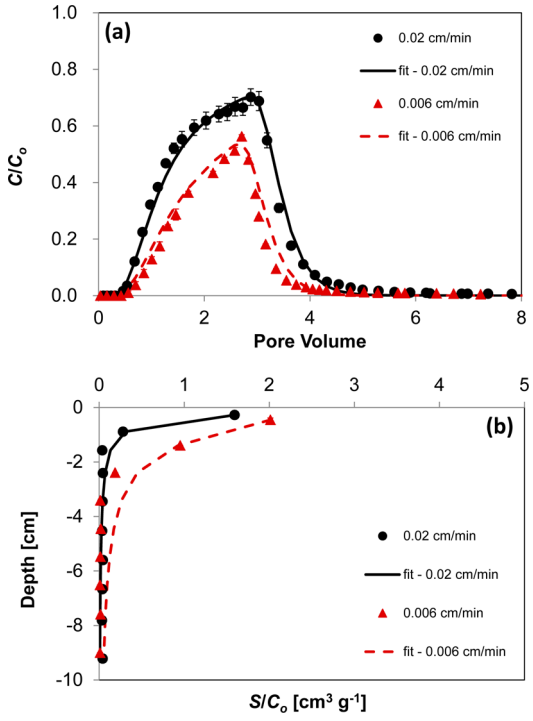

Figure 3. Effect of flow rate on the transport and retention of AgNPs in an undisturbed loamy sand soil: observed and fitted breakthrough curves (a) and retention profiles (b) of AgNPs under Darcy velocity of 0.006 and 0.02 cm/min, respectively. Other experimental conditions were the same: electrolyte, 1 mM KNO_3; input concentration, 10 mg/L AgNPs.

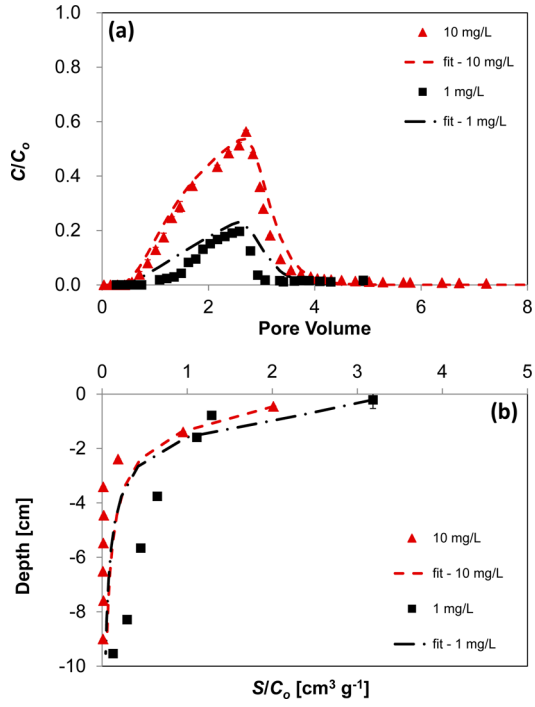

Figure 2. Effect of AgNP concentration on the transport and retention of AgNPs in an undisturbed loamy sand soil: observed and fitted breakthrough curves (a) and retention profiles (b) of AgNPs under AgNP input concentrations of 1 and 10 mg/L, respectively. Other experimental conditions were the same: electrolyte, 1 mM KNO_3; Darcy velocity, 0.006 cm/min.

summarizes the fitted model parameters, the 95% confidence intervals for the fitted parameters, and the Pearson's correlation coefficient (R^2) between observed and simulated data. Overall, the simulated curves were able to capture the main features of AgNP transport and retention ($R^2 > 0.959$).

The BTCs for AgNPs were retarded in comparison with the tracer (data not shown). This retardation is also evident in Figures 1−3. In particular, the center of mass of the AgNP breakthrough front frequently occurred after 1 pore volume. These retarded breakthrough curves can be quantified with the fitted parameters k_1 and S_{max}/C_o in eqs 1−3 which are related to the retention rate and capacity of AgNPs on the porous media, respectively. A high value of k_1 produces complete retention until S_{max}/C_o is filled. Consequently, more retarded BTCs are expected for higher k_1 and larger S_{max}/C_o. However, if k_1 is too low, then breakthrough will occur (no retardation) and the BTC will slowly increase with time as the favorable retention locations are gradually filled.

More retarded BTCs, lower effluent concentrations, and greater retention occurs at higher IS in Figure 1. This can be explained by an increase in k_1 and S_{max}/C_o with IS (SI Table S1) that occurs due to compression of the electrical double layer thickness that produces a shallow secondary minimum and enhances the effects of nanoscale heterogeneities.[41] Higher values of C_o (input concentration) produced less retardation, higher effluent concentrations, and less retention in Figure 2. One potential explanation is due to blocking which increases the rate of filling of S_{max} with a larger C_o.[42] In addition, the retained AgNPs could hinder further retention due to the repulsive AgNP−AgNP interactions especially when more particles were retained at higher C_o.[33] An observed decrease in k_1 and S_{max}/C_o with larger C_o supports this hypothesis (SI

dx.doi.org/10.1021/es402046u | Environ. Sci. Technol. 2013, 47, 12229−12237

Table S1). Higher effluent concentrations and less retention were observed in Figure 3 for higher q (flow velocity). Similar to experimental observations, filtration theory predicts that k_1 is proportional to q to the 1/3 power.[43] However, the overall rate of advection is proportional to q, so a decrease in retention is expected with an increase in q. Experimental values of S_{max}/C_o also decrease with higher q similar to predicted trends when conducting a balance of applied hydrodynamic and resisting adhesive torques to determine the fraction of the solid surface that contributes to colloid immobilization.[41]

The above results indicate that AgNP transport and retention in soil are highly dependent on blocking, which has also been demonstrated to play an important role in homogeneous quartz sand.[33] Similar to Figures 1−3, BTCs for AgNPs in quartz sand were observed to decrease with IS, and to increase with C_o and q. In contrast to Figures 1−3, retardation was not observed to play a significant role in the quartz sands. Furthermore, the RPs in the loamy sand (Figures 1−3) were always hyperexponential in shape and a significant fraction of the retained AgNPs (approximately 70%) was in the top 0−3 cm. In contrast, blocking caused the RP shapes to transition from hyperexponential, to nonmonotonic, and to uniform in the quartz sand.[33] These differences can partially be ascribed to the higher values of S_{max}/C_o in the current work (>1.94 $cm^3\ g^{-1}$). In comparison, values of S_{max}/C_o were frequently as low as 0.732 $cm^3\ g^{-1}$ in the quartz sand.[33] In addition, as confirmed by the BET surface area analysis, the interacting surface area in the loamy sand (1.7 $m^2\ g^{-1}$) is much greater than in the quartz sand (less than 0.2 $m^2\ g^{-1}$). Both of these factors tend to diminish the relative importance of blocking in loamy sand in comparison to quartz sand; e.g., it takes more AgNPs to fill a larger value of S_{max}/C_o.[44,45]

Several explanations have been proposed in the literature for hyperexponential RPs, including: aggregation,[37] straining,[11] chemical heterogeneity on the particle,[45] and system hydrodynamics.[46] These hypotheses will be briefly examined below. Our TEM images taken from the column effluent (SI Figure S2) demonstrated that the AgNPs were still well dispersed. Furthermore, the BTCs did not exhibit ripening behavior (increasing retention rate with time). This information suggests that AgNP aggregation was insignificant during the transport experiments. Straining was neglected because of the small ratio of the AgNP diameter to the soil grain size.[11] Charge heterogeneity on the AgNP surface was an unlikely explanation because the zeta potentials for AgNPs in influent and effluent solutions were very similar. Alternatively, variations in the pore-scale velocity can provide a viable explanation for the hyperexponential RPs when the flux adjacent to the solid surface near the column inlet is the dominant mass transfer mechanism to the solid-water interface.[46] This effect is reported to be more pronounced in finer textured porous media,[46] which is consistent with the higher value of β in eq 3 for AgNPs in loamy sand (β = 1.532) than quartz sand (β = 0.432).[33] A higher value of β indicates a stronger depth dependence of the retention coefficient (k_1).

Liang et al.[33] reported that the AgNPs attached to quartz sand in a weak secondary minimum and a strong primary minimum. Similar interactions are expected for AgNPs in the loamy sand. Secondary minimum interactions are very shallow for AgNPs under low IS conditions.[33] Consequently, the kinetic energy of diffusing AgNPs is expected to be sufficiently large to overcome most of the shallow secondary minimum interactions.[47] Conversely, primary minimum interactions may be significant for nanoparticles as a result of nanoscale chemical and physical heterogeneity on the soil surface.[41] Nanoscale heterogeneity is well-known to be significant for soils due to roughness and adsorbed clays, natural organic matter (NOM), metal oxides, ions, and variations in mineralogy.[48] The nanoscale−scale heterogeneity on the soil surface may produce primary minimum interactions for AgNPs depending of the cross-sectional area of the heterogeneity and the solution IS.[41] However, charge heterogeneity on the soil surface will tend to be masked by NOM[49−51] present in the loamy sand (1.1%)[35] or free surfactant in the AgNP suspension.[33] Furthermore, the effect of nanoscale heterogeneity on AgNP retention is expected to be diminished under low IS conditions.[41] Both of these factors can help to explain the high mobility of AgNPs in the loamy sand when the IS was 1 mM (Figure 1). Collectively, these results suggest that AgNP transport in the loamy sand soil was mainly controlled by primary minimum interactions from soil heterogeneities that were diminished by NOM, especially under low IS conditions.

AgNP Remobilization. Experiments I−IV were conducted to better understand the effect of cation type, IS reduction, and cation exchange on the release of AgNPs in soil. Figure 4 presents BTCs when AgNPs were deposited and eluted (step A) in the presence of KNO_3 or $Ca(NO_3)_2$ at an IS of 10 mM, and then release of AgNPs was initiated in step B by a reduction in IS (Milli-Q water). Retention of AgNPs in step A was more pronounced in the presence of $Ca(NO_3)_2$ than KNO_3, even though the IS was the same. This can be explained by bridging complexation between soil grains and functionalized nanoparticles in the presence of Ca^{2+}.[24] Natural mineral surfaces such as clays are known to show a stronger affinity for divalent than monovalent cations.[16] Release of AgNPs by IS reduction (step B) was more pronounced when the AgNPs were retained (step A) in the presence of monovalent cation. Mass balance information indicates that the recovery in step B was 31.7% for KNO_3 solution and only 16% for $Ca(NO_3)_2$ (Table 1). This behavior indicates that some of the AgNPs were interacting in a reversible minimum that was eliminated by a reduction in the IS. However, the resistance to AgNP release with IS reduction was apparently greater in the presence of $Ca(NO_3)_2$ than KNO_3, suggesting that cation bridging created stronger primary minimum interactions.[5] Our exper-

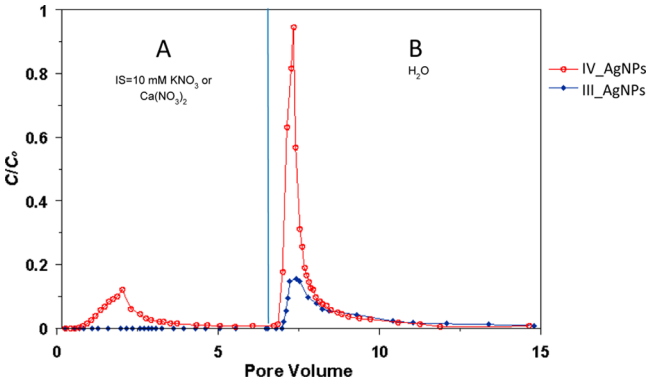

Figure 4. Breakthrough and release behavior of AgNPs in an undisturbed loamy sand soil. Deposition (step A) occurred at an IS = 10 mM using $Ca(NO_3)_2$ (experiment III) or KNO_3 (experiment IV), whereas release (step B) was initiated by eluting with Milli-Q water. The Darcy velocity was 0.02 cm/min and the input AgNP concentration was 10 mg/L.

imental results also indicate that these primary minimum interactions were not diminished by long elution at reduced IS.

Figure 5a shows the AgNP BTCs from experiments I–III in the presence of $Ca(NO_3)_2$ when the IS in step A was 1, 5, and

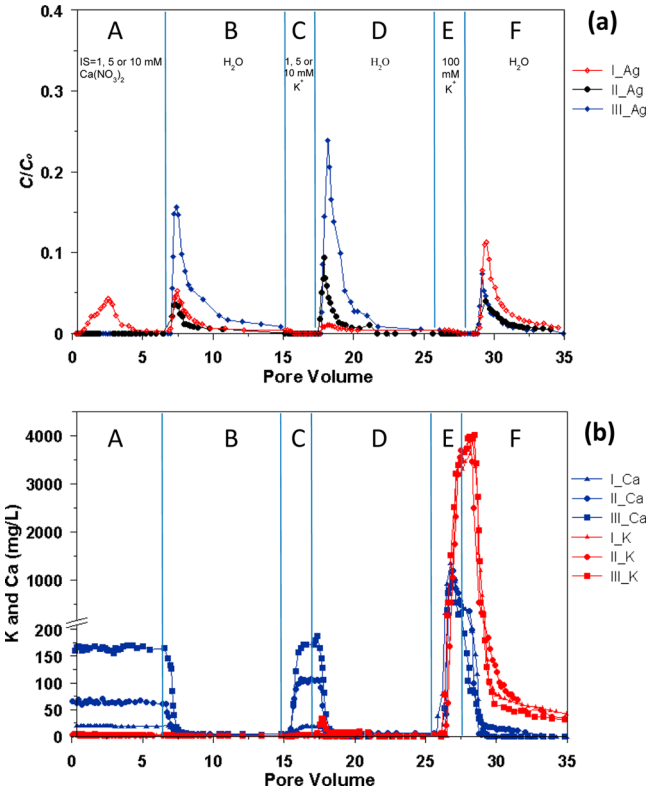

Figure 5. (a) Breakthrough and release behavior of AgNPs in an undisturbed loamy sand soil. Deposition (step A) occurred at an IS = 1, 5, and 10 mM using $Ca(NO_3)_2$ for experiment I, II, and III, respectively, whereas release was initiated by eluting with Milli-Q water (steps B, D, and F) and cation exchange (steps C and E) as summarized in Table 1. (b): Effluent concentrations of K and Ca during steps A–F. The Darcy velocity was 0.02 cm/min and the input AgNP concentration (C_o) was 10 mg/L.

10 mM, respectively. The subsequent release procedures were Milli-Q water (step B), KNO_3 at the same IS as in step A (step C), Milli-Q water (step D), 100 mM KNO_3 (step E), and Milli-Q water (step F). A small amount (3.9%) of the injected AgNPs was transported through the undisturbed soil column during step A in experiment I. In contrast, the AgNP concentrations in the effluent from step A were under the detection limit in experiments II and III. The recoveries of AgNPs in step B (Milli-Q water) were 3.8%, 4.6%, and 16.0% for experiment I, II, and III, respectively. Similar to Figure 1, these observations suggests that a greater amount of AgNPs were reversibly retained in a secondary minimum with the higher IS in step A.

When KNO_3 was introduced in step C at the same IS as in step A and at a much larger IS of 100 mM in step E, further AgNP remobilization occurred by IS reduction in steps D and F. The continued release of AgNPs as IS reduced during steps D and F was initiated by the cation exchange during steps C and E, respectively. Figure 5b shows plots of K^+ and Ca^{2+} concentrations in the column effluent for experiments I–III. Around 95% of the injected K^+ mass in step C was retained in the column even after flushing with Milli-Q water during step D. Conversely, less than 20% of the injected K^+ (100 mM) in step E was adsorbed to the soil and high release peaks for Ca^{2+} were observed. This clearly indicates that excess amounts of K^+ in step E produced substantial release of Ca^{2+} as a result of cation exchange. However, very little AgNP release occurred during cation exchange (C and E), while rather significant release of AgNPs occurred during IS reduction (D and F) immediately following cation exchange. Exchange of K^+ for Ca^{2+} will decrease the potential for bridging complexation, whereas IS reduction will expand the double layer thickness and eliminate the secondary minimum. These observations suggest that both cation exchange and IS reduction were needed to release the AgNPs that were interacting with the soil grains in the presence of divalent cation.

The amount of AgNPs that were released in step D followed a similar trend to that shown in step B (Table 1); e.g., increasing with IS of KNO_3 in step C. This observation suggests that IS reduction was the dominant cause of release in this case. Conversely, greater amounts of AgNP release occurred in step F for soils exposed to lower concentrations of $Ca(NO_3)_2$ during step A (Table 1). Consequently, a larger amount of AgNPs was released when the cation exchange was more pronounced followed by IS reduction. Bradford and Kim[52] observed significant amounts of kaolinite clay release following similar processes of cation exchange (Na^+ for Ca^{2+}) and IS reduction. Similarly, the effluent was very turbid during steps B, D, and F. This phenomenon implied the release of natural soil colloids from the loamy sand soil. The remobilization of soil colloids from an AgNP-free soil column was confirmed by measuring effluent concentrations of Al and Fe shown in SI Figure S3. Notice that the release of Al and Fe in soil showed a very similar trend as the release of AgNPs (Figure 5a), suggesting the potential for AgNP association with soil colloids. Additional evidence for the role of soil colloids on AgNP release is provided below.

To further confirm the potential for soil colloids to facilitate the release of AgNPs, Figure 6a presents plots of Ag, Al, and Fe concentration for steps A–F. In this case, AgNP deposition and elution during step A occurred in the presence of $Ca(NO_3)_2$ at an IS of 5 mM when C_o was 10 mg/L and q was 0.7 cm/min. In contrast to other experiments, a repacked soil column was employed under saturated conditions because all of the undisturbed soil columns had already been used. Similar to SI Figure S3, the release of AgNPs was highly correlated with Fe and Al concentrations of soil colloids. The association of AgNPs with soil colloids was further confirmed by TEM investigation. Figure 6b,c presents representative TEM images of soil colloids in the effluent. The black dots on these colloids were confirmed by EDX to be AgNPs (Figure 6d,e). A rigorous determination of the colloid-associated fraction of AgNPs was not attempted because of TEM limitations in sample preparation and inspection, and the transient solution chemistry conditions. Nevertheless, the TEM images (Figure 6b,c) and EDX analysis (Figures 6d,e), correlations between Ag, Fe, and Al (SI Figures S3 and 6a), and available literature[48,53] do support the interaction between soil colloids and some fraction of the released AgNPs. Additional research is needed to fully resolve the role of soil colloids (such as clay minerals, iron oxide-hydroxide, and their complexes) in facilitating the release and transport of AgNPs during transient solution chemistry conditions.

Environmental Implications. Experiments were designed to examine the effects of physicochemical factors (IS, cation

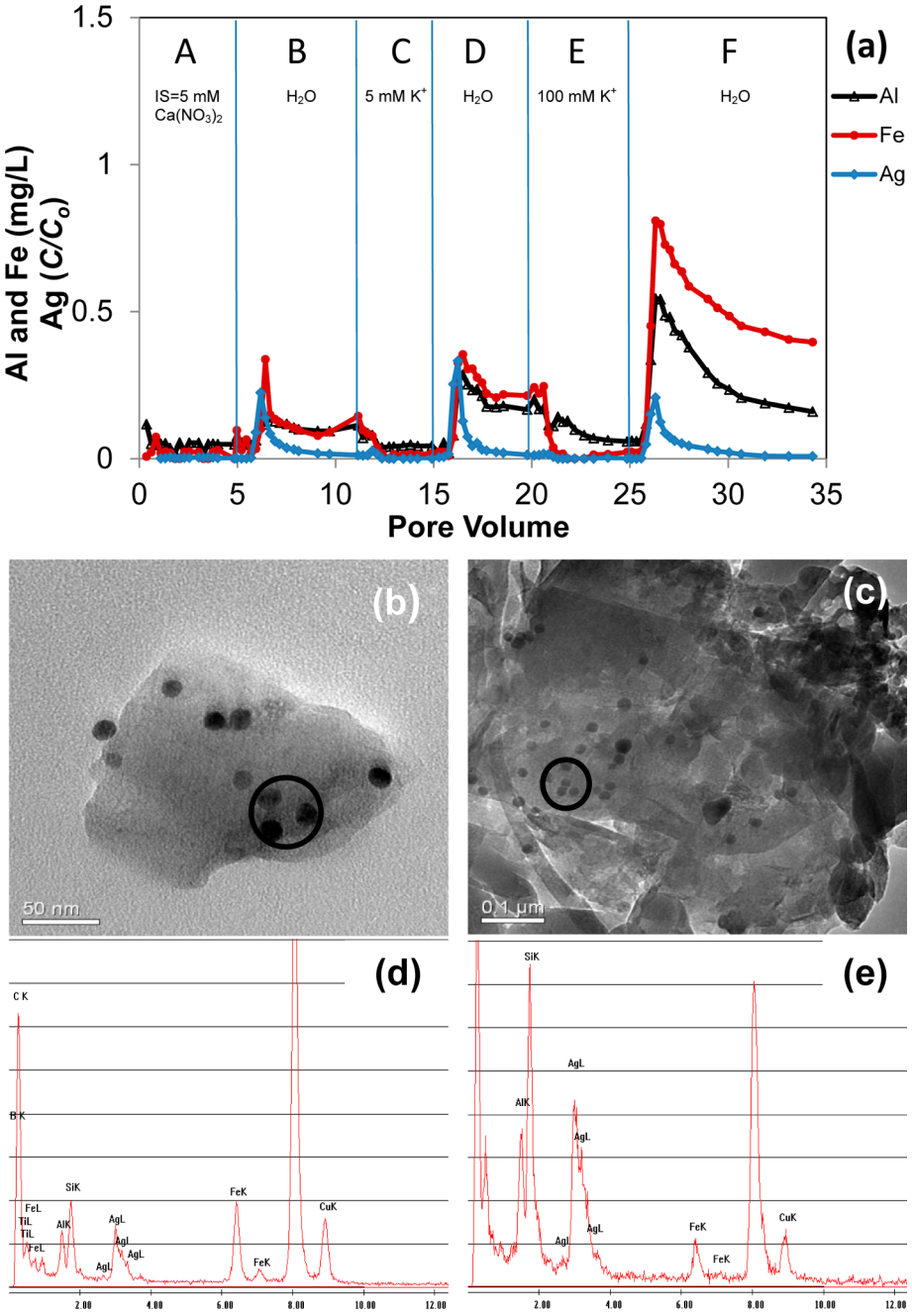

Figure 6. (a) Release of AgNPs and naturally occurring minerals by cation exchange (steps C and E) and ionic strength reduction (steps B, D, and F) in a saturated, repacked soil column. The Darcy velocity was 0.7 cm/min and the input AgNP concentration (C_o) was 10 mg/L. (b)–(e): Transmission electron microscopy (b and c) and energy-dispersive X-ray spectroscopy (EDX) (d and e) measurements of AgNPs in the effluent sampled from release experiment after cation exchange (AgNPs cotransported through soil column with released naturally occurring colloids/clay). The marked points in (b) and (c) were selected for EDX analysis as shown in (d) and (e), respectively.

type, C_o, and q) on the transport, retention, and release of surfactant stabilized AgNPs in undisturbed soil, near water saturation (90%) conditions to represent the maximum transport potential in the vadose zone. Similar to column studies conducted with repacked quartz sand,[33] the mobility of the AgNPs was highly dependent on the physicochemical conditions. In contrast, the BTCs for AgNPs in the undisturbed loamy sand exhibited significant amounts of retardation and the shape of the RPs was hyperexponential. The amount of retardation was dependent on physicochemical properties that influenced the retention rate and/or capacity. Release of AgNPs and soil colloids was promoted by a reduction in IS, monovalent ions, and cation exchange. An association between some fraction of the released AgNPs and soil colloids was also observed. Collectively, our results demonstrate that AgNP transport studies in field soils need to consider retarded BTCs, hyperexponential RPs, cation exchange, and colloid associations which are commonly neglected in repacked sand column experiments. The release processes can produce significant amounts of AgNP migration that pose a potential risk of groundwater contamination during intermittent rain and

irrigation events that produce transient changes in solution chemistry.

■ ASSOCIATED CONTENT

Supporting Information

Brief description and discussion of the following: (i) characterization of AgNPs; (ii) procedures for collecting undisturbed soil samples and for running the column experiments; (iii) fitted values of k_1 and S_{max}/C_o (Table S1); (iv) zeta potentials of the soil grains as a function of KNO_3 and $Ca(NO_3)_2$ concentrations (Figure S1); (v) transmission electron micrograph of AgNPs in effluent (Figure S2); and (vi) release of Fe and Al from a AgNP-free soil column by cation exchange and IS reduction (Figure S3). This material is available free of charge via the Internet at http://pubs.acs.org.

■ AUTHOR INFORMATION

Corresponding Author

*Phone: +1 951 369 4857; fax: +1 951 342 4964; e-mail: scott.bradford@ars.usda.gov.

Notes

The authors declare no competing financial interest.

■ ACKNOWLEDGMENTS

The first author thanks the China Scholarship Council (CSC) for financial support. This research was funded by the NanoFlow project supported by German Federal Ministry of Education and Research (BMBF). The authors would like to acknowledge Ansgar Weuthen and Claudia Walraf for the technical assistance, and Michael Burkhardt for valuable suggestions.

■ REFERENCES

(1) Nowack, B.; Bucheli, T. D. Occurrence, behavior and effects of nanoparticles in the environment. *Environ. Pollut.* **2007**, *150* (1), 5−22.

(2) Song, J. E.; Phenrat, T.; Marinakos, S.; Xiao, Y.; Liu, J.; Wiesner, M. R.; Tilton, R. D.; Lowry, G. V. Hydrophobic interactions increase attachment of gum arabic- and PVP-coated Ag nanoparticles to hydrophobic surfaces. *Environ. Sci. Technol.* **2011**, *45* (14), 5988−5995.

(3) Wang, Y.; Li, Y.; Costanza, J.; Abriola, L. M.; Pennell, K. D. Enhanced mobility of fullerene (C_{60}) Nanoparticles in the presence of stabilizing agents. *Environ. Sci. Technol.* **2012**, *46* (21), 11761−11769.

(4) Kasel, D.; Bradford, S. A.; Šimůnek, J.; Heggen, M.; Vereecken, H.; Klumpp, E. Transport and retention of multi-walled carbon nanotubes in saturated porous media: Effects of input concentration and grain size. *Water Res.* **2013**, *47* (2), 933−944.

(5) Jaisi, D. P.; Saleh, N. B.; Blake, R. E.; Elimelech, M. Transport of single-walled carbon nanotubes in porous media: Filtration mechanisms and reversibility. *Environ. Sci. Technol.* **2008**, *42* (22), 8317−8323.

(6) Jaisi, D. P.; Elimelech, M. Single-walled carbon nanotubes exhibit limited transport in soil columns. *Environ. Sci. Technol.* **2009**, *43* (24), 9161−9166.

(7) Sagee, O.; Dror, I.; Berkowitz, B. Transport of silver nanoparticles (AgNPs) in soil. *Chemosphere* **2012**, *88* (5), 670−675.

(8) Ko, C.-H.; Elimelech, M. The "shadow effect" in colloid transport and deposition dynamics in granular porous media: Measurements and mechanisms. *Environ. Sci. Technol.* **2000**, *34* (17), 3681−3689.

(9) Adamczyk, Z.; Siwek, B.; Szyk, L. Flow-induced surface blocking effects in adsorption of colloid particles. *J. Colloid Interface Sci.* **1995**, *174* (1), 130−141.

(10) Yao, K.-M.; Habibian, M. T.; O'Melia, C. R. Water and waste water filtration. Concepts and applications. *Environ. Sci. Technol.* **1971**, *5* (11), 1105−1112.

(11) Li, X.; Scheibe, T. D.; Johnson, W. P. Apparent decreases in colloid deposition rate coefficients with distance of transport under unfavorable deposition conditions: A general phenomenon. *Environ. Sci. Technol.* **2004**, *38* (21), 5616−5625.

(12) Tong, M.; Li, X.; Brow, C. N.; Johnson, W. P. Detachment-influenced transport of an adhesion-deficient bacterial strain within water-reactive porous media. *Environ. Sci. Technol.* **2005**, *39* (8), 2500−2508.

(13) Bergendahl, J.; Grasso, D. Prediction of colloid detachment in a model porous media: Hydrodynamics. *Chem. Eng. Sci.* **2000**, *55* (9), 1523−1532.

(14) Ryan, J. N.; Elimelech, M. Colloid mobilization and transport in groundwater. *Colloids Surf., A* **1996**, *107* (0), 1−56.

(15) Tufenkji, N.; Elimelech, M. Deviation from the classical colloid filtration theory in the presence of repulsive DLVO interactions. *Langmuir* **2004**, *20* (25), 10818−10828.

(16) Roy, S. B.; Dzombak, D. A. Colloid release and transport processes in natural and model porous media. *Colloids Surf., A* **1996**, *107* (0), 245−262.

(17) Liu, X.; O'Carroll, D. M.; Petersen, E. J.; Huang, Q.; Anderson, C. L. Mobility of multiwalled carbon nanotubes in porous media. *Environ. Sci. Technol.* **2009**, *43* (21), 8153−8158.

(18) Chen, G.; Flury, M. Retention of mineral colloids in unsaturated porous media as related to their surface properties. *Colloids Surf., A* **2005**, *256* (2−3), 207−216.

(19) Mishurov, M.; Yakirevich, A.; Weisbrod, N. Colloid transport in a heterogeneous partially saturated sand column. *Environ. Sci. Technol.* **2008**, *42* (4), 1066−1071.

(20) Sirivithayapakorn, S.; Keller, A. Transport of colloids in unsaturated porous media: A pore-scale observation of processes during the dissolution of air-water interface. *Water Resour. Res.* **2003**, *39* (12), 1346.

(21) Kjaergaard, C.; Poulsen, T. G.; Moldrup, P.; de Jonge, L. W. Colloid mobilization and transport in undisturbed soil columns. I. Pore structure characterization and tritium transport. *Vadose Zone J.* **2004**, *3* (2), 413−423.

(22) Huynh, K. A.; Chen, K. L. Aggregation kinetics of citrate and polyvinylpyrrolidone coated silver nanoparticles in monovalent and divalent electrolyte solutions. *Environ. Sci. Technol.* **2011**, *45* (13), 5564−5571.

(23) Badawy, A. M. E.; Luxton, T. P.; Silva, R. G.; Scheckel, K. G.; Suidan, M. T.; Tolaymat, T. M. Impact of environmental conditions (pH, ionic strength, and electrolyte type) on the surface charge and aggregation of silver nanoparticles suspensions. *Environ. Sci. Technol.* **2010**, *44* (4), 1260−1266.

(24) Torkzaban, S.; Wan, J.; Tokunaga, T. K.; Bradford, S. A. Impacts of bridging complexation on the transport of surface-modified nanoparticles in saturated sand. *J. Contam. Hydrol.* **2012**, *136−137*, 86−95.

(25) Lin, S.; Cheng, Y.; Bobcombe, Y.; L. Jones, K.; Liu, J.; Wiesner, M. R. Deposition of silver nanoparticles in geochemically heterogeneous porous media: Predicting affinity from surface composition analysis. *Environ. Sci. Technol.* **2011**, *45* (12), 5209−5215.

(26) Thio, B. J. R.; Montes, M. O.; Mahmoud, M. A.; Lee, D.-W.; Zhou, D.; Keller, A. A. Mobility of capped silver nanoparticles under environmentally relevant conditions. *Environ. Sci. Technol.* **2012**, *46* (13), 6985−6991.

(27) Kim, B.; Park, C.-S.; Murayama, M.; Hochella, M. F. Discovery and characterization of silver sulfide nanoparticles in final sewage sludge products. *Environ. Sci. Technol.* **2010**, *44* (19), 7509−7514.

(28) Nowack, B. Nanosilver revisited downstream. *Science* **2010**, *330* (6007), 1054−1055.

(29) Levard, C.; Hotze, E. M.; Lowry, G. V.; Brown, G. E. Environmental transformations of silver nanoparticles: Impact on stability and toxicity. *Environ. Sci. Technol.* **2012**, *46* (13), 6900−6914.

(30) Li, X.; Lenhart, J. J. Aggregation and dissolution of silver nanoparticles in natural surface water. *Environ. Sci. Technol.* **2012**, *46* (10), 5378−5386.

(31) El Badawy, A. M.; Aly Hassan, A.; Scheckel, K. G.; Suidan, M. T.; Tolaymat, T. M. Key factors controlling the transport of silver nanoparticles in porous media. *Environ. Sci. Technol.* **2013**, *47* (9), 4039−4045.
(32) Lin, S.; Cheng, Y.; Liu, J.; Wiesner, M. R. Polymeric coatings on silver nanoparticles hinder autoaggregation but enhance attachment to uncoated surfaces. *Langmuir* **2012**, *28* (9), 4178−4186.
(33) Liang, Y.; Bradford, S. A.; Simunek, J.; Vereecken, H.; Klumpp, E. Sensitivity of the transport and retention of stabilized silver nanoparticles to physicochemical factors. *Water Res.* **2013**, *47* (7), 2572−2582.
(34) Jacobsen, O. H.; Moldrup, P.; Larsen, C.; Konnerup, L.; Petersen, L. W. Particle transport in macropores of undisturbed soil columns. *J. Hydrol.* **1997**, *196* (1−4), 185−203.
(35) Unold, M.; Simunek, J.; Kasteel, R.; Groeneweg, J.; Vereecken, H. Transport of manure-based applied sulfadiazine and its main transformation products in soil columns. *Vadose Zone J.* **2009**, *8* (3), 677−689.
(36) Förster, M.; Laabs, V.; Lamshöft, M.; Pütz, T.; Amelung, W. Analysis of aged sulfadiazine residues in soils using microwave extraction and liquid chromatography tandem mass spectrometry. *Anal. Bioanal. Chem.* **2008**, *391* (3), 1029−1038.
(37) Bradford, S. A.; Simunek, J.; Walker, S. L. Transport and straining of *E. coli* O157:H7 in saturated porous media. *Water Resour. Res.* **2006**, *42* (12), W12S12.
(38) Deshpande, P. A.; Shonnard, D. R. Modeling the effects of systematic variation in ionic strength on the attachment kinetics of Pseudomonas fluorescens UPER-1 in saturated sand columns. *Water Resour. Res.* **1999**, *35* (5), 1619−1627.
(39) Marquardt, D. W. An algorithm for least-squares estimation of nonlinear parameters. *J. Soc. Ind. Appl. Math.* **1963**, *11* (2), 431−441.
(40) Šimůnek, J.; Genuchten, M. T. v.; Šejna, M. Development and applications of the HYDRUS and STANMOD software packages, and related codes. *Vadose Zone J.* **2008**, *7* (2), 587−600.
(41) Bradford, S. A.; Torkzaban, S. Colloid interaction energies for physically and chemically heterogeneous porous media. *Langmuir* **2013**, *29* (11), 3668−3676.
(42) Bradford, S. A.; Kim, H. N.; Haznedaroglu, B. Z.; Torkzaban, S.; Walker, S. L. Coupled factors influencing concentration-dependent colloid transport and retention in saturated porous media. *Environ. Sci. Technol.* **2009**, *43* (18), 6996−7002.
(43) Schijven, J. F.; Hassanizadeh, S. M. Removal of viruses by soil passage: Overview of modeling, processes, and parameters. *BEST* **2000**, *30* (1), 49−127.
(44) Tong, M.; Johnson, W. P. Colloid population heterogeneity drives hyperexponential deviation from classic filtration theory. *Environ. Sci. Technol.* **2006**, *41* (2), 493−499.
(45) Tufenkji, N.; Elimelech, M. Breakdown of colloid filtration theory: Role of the secondary energy minimum and surface charge heterogeneities. *Langmuir* **2005**, *21* (3), 841−852.
(46) Bradford, S. A.; Torkzaban, S.; Simunek, J. Modeling colloid transport and retention in saturated porous media under unfavorable attachment conditions. *Water Resour. Res.* **2011**, *47* (10), W10503.
(47) Shen, C.; Li, B.; Huang, Y.; Jin, Y. Kinetics of coupled primary- and secondary-minimum deposition of colloids under unfavorable chemical conditions. *Environ. Sci. Technol.* **2007**, *41* (20), 6976−6982.
(48) Cornelis, G.; DooletteMadeleine Thomas, C.; McLaughlin, M. J.; Kirby, J. K.; Beak, D. G.; Chittleborough, D. Retention and dissolution of engineered silver nanoparticles in natural soils. *Soil Sci. Soc. Am. J.* **2012**, *76* (3), 891−902.
(49) Pan, B.; Xing, B. Applications and implications of manufactured nanoparticles in soils: a review. *Eur. J. Soil Sci.* **2012**, *63* (4), 437−456.
(50) Lecoanet, H. F.; Bottero, J.-Y.; Wiesner, M. R. Laboratory assessment of the mobility of nanomaterials in porous media. *Environ. Sci. Technol.* **2004**, *38* (19), 5164−5169.
(51) Badawy, A. E., Assessment of the Fate and Transport of Silver Nanoparticles in Porous Media. Ph.D. Dissertation, University of Cincinnati: Cincinnati, OH, 2011.
(52) Bradford, S. A.; Kim, H. Implications of cation exchange on clay release and colloid-facilitated transport in porous media. *J. Environ. Qual.* **2010**, *39* (6), 2040−2046.
(53) Zhou, D.; Abdel-Fattah, A. I.; Keller, A. A. Clay particles destabilize engineered nanoparticles in aqueous environments. *Environ. Sci. Technol.* **2012**, *46* (14), 7520−7526.